Cooperative Microbial Interactions Mediate Community Biogeochemical Responses to Saltwater Intrusion in Wetland Soils

David J. Berrier, Scott C. Neubauer, and Rima B. Franklin[#]

Department of Biology

Virginia Commonwealth University

1000 W Cary Street

Richmond, Virginia 23284

(USA)

[#] Author for correspondence

rbfranklin@vcu.edu

Telephone: 804-828-6753

Key words: methanogens, syntrophy, sulfate-reducing bacteria, saltwater intrusion, tidal freshwater wetland, sea level rise

ABSTRACT

In freshwater wetlands, competitive and cooperative interactions between respiratory, fermentative, and methanogenic microbes mediate the decomposition of organic matter. These interactions may be disrupted by saltwater intrusion disturbances that enhance the activity of sulfate-reducing bacteria (SRB), intensifying their competition with syntrophic bacteria and methanogens for electron donors. We simulated saltwater intrusion into wetland soil microcosms and examined biogeochemical and microbial responses, employing metabolic inhibitors to isolate the activity of various microbial functional groups. Sulfate additions increased total carbon dioxide production but decreased methane production. Butyrate degradation assays showed continued (but lower) levels of syntrophic metabolism despite strong demand by SRB for this key intermediate decomposition product and a shift in the methanogen community toward acetoclastic members. One month after removing SRB competition, total methane production recovered by only ~50%. Similarly, butyrate assays showed an altered accumulation of products (including less methane), although overall rates of syntrophic butyrate breakdown largely recovered. These effects illustrate that changes in carbon mineralization following saltwater intrusion are driven by more than the oft-cited competition between SRB and methanogens for shared electron donors. Thus, the impacts of disturbances on wetland biogeochemistry are likely to persist until cooperative and competitive microbial metabolic interactions can recover fully.

INTRODUCTION

In freshwater wetland soils, a complex, interacting consortium of microorganisms mediates the decomposition of organic matter through a series of respiratory and fermentative pathways, resulting in the production of carbon dioxide (CO_2) and methane (CH_4) (Megonigal *et al.* 2004). Primary fermentation breaks large organic molecules into a variety of low molecular weight acids and alcohols, which are mineralized by microbes using inorganic terminal electron acceptors (e.g., NO_3^-, Fe(III), SO_4^{2-}) or which serve as substrates for secondary fermentation and methanogenesis. The processes that ultimately result in the production of CH_4 often rely on cooperative interspecies metabolic interactions (i.e., syntrophy) between methanogenic archaea and syntrophic bacteria (that is, fermentative bacteria that require a metabolic partner). For example, the fermentative breakdown of many of the products of primary fermentation (e.g., butyrate and propionate) is only made thermodynamically possible when electron carrier molecules (e.g., H_2 and/or formate) produced by syntrophic bacteria are rapidly consumed and maintained at low concentrations by hydrogenotrophic methanogens (McInerney *et al.* 2009; Stams and Plugge 2009) (Fig. 1). The rapid consumption of these electron carrier molecules is often enhanced by the close proximity of syntrophic bacteria and hydrogenotrophic methanogens in aggregates (De Bok *et al.* 2004; Stams and Plugge 2009). The interactions between syntrophic bacteria and methanogens can be integral in the regulation of methanogenesis and organic matter decomposition in freshwater wetland soils and other anaerobic environments (Conrad *et al.* 1989; Bae and McCarty 1993; Stefanie *et al.* 1994; McInerney *et al.* 2009).

Environmental disturbances can change the quantity and quality of organic matter, impact the availability of microbially-relevant ions, and otherwise modify the physicochemical properties of wetland soils, leading to reshuffled interactions between members of the microbial community and altered rates of methanogenesis and carbon cycling. One such disturbance experienced by freshwater wetlands is the increasing frequency and duration of episodic saltwater intrusion events due to sea level rise and climate change (Neubauer and Craft 2009; Moftakhari *et al.* 2015), which lead to increases in ionic strength and greater availability of the electron acceptor sulfate (SO_4^{2-}) (Herbert *et al*. 2015; Tully *et al.* 2019). Saltwater intrusion therefore has the potential to alter the syntrophic breakdown of butyrate. In both freshwater and saline environments, many organic matter decomposition pathways include butyrate as an intermediate (Parkes *et al.* 1989; Rothfuss and Conrad 1992; Glissmann and Conrad 2000; Chauhan *et al.* 2006, Galand *et al.* 2010). In freshwater wetlands, the only known genera capable of syntrophic butyrate breakdown – *Syntrophomonas* and *Syntrophus* – are both obligate syntrophs (McInerney *et al.* 2008; Plugge *et al.* 2011). However, in saline environments where SO_4^{-2} is typically abundant, sulfate-reducing bacteria (SRB) can thrive and may outcompete butyrate-consuming syntrophs, thereby reducing rates of methanogenesis and enhancing the production of CO_2 at the expense of CH_4. In addition to competing with syntrophic bacteria for butyrate, SRB can directly compete with methanogens for electron donors like H_2, formate, and acetate (Stams 1994; Muyzer and Stams 2008; Chambers *et al.* 2011) (Fig. 1), further suppressing rates of CH_4 production.

Across estuarine salinity gradients, there is widely-observed pattern of lower rates of methanogenesis and CH_4 emissions to the atmosphere in salt marshes compared with

freshwater and low-salinity tidal wetlands (Odum 1988; Poffenbarger *et al.* 2011). This is often explained as the thermodynamically-predictable outcome of microbial competition between SRB and methanogens (Lovley *et al.* 1982; Hoehler *et al.* 2001; Tobias and Neubauer 2019), but an additional and unstudied possibility is that higher salinity and SO_4^{2-} concentrations alter the competitive interactions between SRB and the syntroph–methanogen consortia. Further, since saltwater intrusion can be an episodic phenomenon, the resiliency of syntroph–methanogen relationships to this stressor may be important in determining the degree to which rates and pathways of carbon cycling recover once freshwater conditions return. The goals of this study were to investigate the following questions: (i) does SRB competition disrupt the syntroph–methanogen consortia breaking down butyrate, and (ii) do syntroph–methanogen activity and carbon mineralization rates recover after SRB competition is removed. We addressed these questions by measuring total CH_4 and CO_2 production rates, the accumulation of metabolic products following additions of butyrate, and methanogen abundances in freshwater wetland soil microcosms, both before and after additions of SO_4^{2-} or NaCl to simulate saltwater intrusion and the application of selective metabolic inhibitors to isolate the role of individual microbial groups on carbon mineralization.

METHODS

Microcosm setup

This study focused on Cumberland Marsh (latitude: 37.55723 ° N, longitude: 76.97277 ° W), a tidal freshwater wetland located on the Pamunkey River in Virginia (USA). The site has been the subject of several prior studies investigating the effects of

saltwater intrusion on wetland microbial communities (Dang et al., 2020; Morrissey and Franklin 2015). It experiences consistently low salinity (<0.5 PSU) and has a plant community dominated by obligate freshwater macrophytes such as *Peltandra virginica* (arrow arum) and *Pontederia cordata* (pickerelweed).

The soil used for this experiment was collected on 1 October 2015, during low tide, by first pushing aside the consolidated layer of plant debris and then carefully transferring the top 5 cm to an airtight plastic bag. The process was repeated at several locations across two 40-m transects, and the soil samples were combined (~3 kg total). Our decision to focus on near-surface soil was motivated by prior research showing rates of microbial activity (i.e., CO_2 and CH_4 production) to be highest in this region (Neubauer et al., 2013); therefore, this is where saltwater-induced disruptions to syntroph–methanogen interactions would be most easily detected and consequential. The resultant soil had a gravimetric moisture content of ~85%, a redox potential of -130 mV, a bulk density of ~0.2 g cm^{-3}, and an organic matter content of 35%. In addition, ~10 L of porewater was collected from the marsh by digging several small pits, emptying them of standing water, and then allowing them to naturally refill. The salinity of this porewater was <0.1 PSU (conductivity <0.2 mS cm^{-1}).

Upon return to the lab, porewater was deoxygenated (1 hr with N_2) and then mixed with the composite soil sample to create ~9 L of bulk slurry (30 g wet soil per 100 ml porewater). The slurry was manually homogenized, filtered through a 2.38 mm sieve to remove roots, and then aliquoted (100 ml) into glass serum bottles (170 ml). The serum bottles were sealed with snap-on natural red rubber septa (13 × 20 mm, Wheaton Industries, Millville, New Jersey, USA) and crimped with an aluminum seal. These

microcosms were pre-incubated in the dark at 25 °C for 22 days to allow the microbial communities to stabilize and deplete inorganic terminal electron acceptors (e.g., NO_3^-, Fe(III)) so the experiment could focus on the interactions between methanogens, and SRB with minimal interference from other microbial groups (e.g., denitrifiers, iron reducing bacteria) that might also be able to consume butyrate, formate, and/or acetate. All microcosm preparations and subsequent samplings took place inside an anaerobic chamber that was continually flushed with N_2.

Experimental design

After the pre-incubation period, a subset of microcosms was destructively sampled to characterize the "initial" conditions prior to any treatment manipulations (Fig. 2). For this sampling event, we measured soil properties, carbon mineralization rates, and archaea abundance (detailed in the "Bulk soil slurry analysis" section below) and performed a series of butyrate degradation assays (detailed in the "Butyrate Assays" section) to study breakdown pathways (Fig. 1).

The remaining microcosms were randomly assigned to become fresh controls (no change) or to experience simulated saltwater intrusion via addition of either Na_2SO_4 or NaCl (Fig. 2). The addition of Na_2SO_4, hereafter referred to as the SO_4^{-2} treatment, was designed to stimulate SRB activity in order to study competitive interactions between SRB, methanogens, and syntrophic bacteria. The concentration of SO_4^{-2} was brought to 4 mM (versus <0.04 mM in fresh control microcosms) to mimic SO_4^{-2} availability in oligohaline waters (0.5 - 5 PSU; 1 - 9 mS cm^{-1}) (Weston et al. 2011). The NaCl treatment was designed to mimic the ionic strength increase that accompanied the Na_2SO_4 addition

(12 mM) and allowed us to disentangle responses associated with increased concentrations of dissolved ions vs. responses specifically due to SO_4^{-2} availability. All microcosms were then incubated for 25 days until the "intrusion" sampling event (Fig. 2), when a subset of microcosms from each treatment was removed for bulk soil slurry analysis and butyrate assays.

Immediately following the "intrusion" sampling event, half of the remaining SO_4^{-2} treatment microcosms were supplemented with Na_2MoO_4 (final concentration of 2.5 mM MoO_4^{-2}) to create a "recovery" treatment. Molybdate is well established as an inhibitor of SRB (Elshahed and McInerney 2001) and its addition allowed us to study how methanogens and syntrophic bacteria recovered once SRB competition was removed. The remaining microcosms were allowed to incubate for an additional 28 days until the "recovery" sampling event. Sufficient microcosms were established at the start of the experiment to allow five replicates for bulk soil slurry analysis for each treatment and time point, and three replicates for each inhibitor addition in the corresponding butyrate assays.

Analysis of bulk soil slurries

At each sampling event, five microcosms from each treatment were destructively sampled to determine carbon mineralization rates (CO_2 and CH_4 production), soil pH, salinity, and archaea abundance. These microcosms are referred to as "bulk soil slurries" throughout the paper to distinguish them from microcosms used in butyrate assays (described below). Rates of CH_4 and CO_2 production were measured using methods similar to Neubauer *et al.* (2005). First, each microcosm was shaken and the headspace

flushed with N_2 gas for 30 minutes. Gas samples were collected 4-5 times over the next ~48 hr by injecting 8 ml of N_2 gas and immediately withdrawing an equal volume from the headspace with a needle and air-tight syringe. Gas samples were stored in 3 ml Labco Exetainers® (Lampeter, Ceredigion, United Kingdom) and later analyzed on a Shimadzu GC-2014 gas chromatograph (Shimadzu Scientific Instruments, Columbia, Maryland, USA); CH_4 was measured with a flame ionization detector and CO_2 was measured with a thermal conductivity detector (Shimalite Q column, He carrier; Shinwa Chemical Industries Ltd., Fushimi-ku, Kyoto, Japan).

After the gas sampling was complete, the microcosms were opened and the contents were transferred to a sterile plastic bag. The pH and conductivity of the soil slurries were then measured using a SevenGo Duo pro Model SG78 meter (Mettler Toledo, Columbus, Ohio, USA). Soil slurries were immediately transferred to a -80 °C freezer for storage until DNA extraction could be performed using the MoBio PowerSoil DNA Isolation Kit following manufacturer's instructions (Carlsbad, California, USA).

These DNA extracts were analyzed using quantitative PCR (qPCR) targeting conserved regions of the *16S rRNA* gene. Using the primer pair Arch967F (5'AAT TGG CGG GGG AGC AC 3') and Arch1060R (5' GGC CAT GCA CCW CCT CTC 3')(Karlson *et al.* 2012), we targeted total archaea, which is the domain where all methanogen species are located (Ferry 2010); we considered abundance of this gene as a proxy for methanogen abundance. We also measured the abundance of the family *Methanosaetaceae* (MST), which encompass all known obligate acetoclastic methanogens (Ferry 2010), using Mst702F (5' TAA TCC TYG ARG GAC CAC CA 3') and Mst862R (5' CCT ACG GCA CCR ACM AC 3')(Yu *et al.* 2005). Acetoclastic

methanogens directly convert acetate to CO_2 and CH_4 and are generally not considered part of the syntropic consortium. Thus, by calculating the ratio of MST 1*6S rRNA* genes copies to archaea *16S rRNA* gene copies, we were able to estimate the fraction of the methanogen community that are not involved in syntrophy.

All qPCR reactions (15 µl, using 4 ng template DNA) were run in triplicate using SsoAdvanced SYBR Green qPCR Supermix (BioRad, Hercules, California, USA) and a Bio-Rad CFX384™Real-Time System C1000 thermal cycler; data were analyzed using Bio-Rad CFX Manager 3.1. Standard curves were constructed with environmental clones (whose sequences had been confirmed) generated from amplicons using the above primers and a pGEM®-T Easy Vector System II (Promega; Madison, Wisconsin, USA). Reaction mixtures targeting total archaea included 0.3 µM of each primer; the thermal cycling conditions were: 95 °C for 10 min followed by 40 cycles of 15 s at 95 °C and 1 min at 60 °C (efficiency = 101 %, r^2 = 0.99). Reaction mixtures targeting MST included 0.5 µM of each primer and used the following thermal cycler conditions: 95 °C for 10 min followed by 45 cycles of 10 s at 94 °C and 30 s at 60 °C (efficiency = 90 %, r^2 = 0.99). In all instances, products were confirmed by examining the melt curve.

Butyrate assays

To investigate the breakdown of butyrate and its byproducts (Fig. 1), an additional subset of microcosms was selected at each sampling event to receive butyrate additions to a final concentration of 2.5 mM (Fig. 2). These microcosms were then divided into groups (n=3 in each) to study the activity of various microbial functional groups using metabolic inhibitors: methanogens were inhibited using 50 mM BESA (Liu *et al.* 2011),

SRB were inhibited using 2.5 mM Na_2MoO_4 (Elshahed and McInerney 2001), and syntrophs were inhibited by adding H_2 every other day to a partial pressure greater than 1.5 kPa (Dwyer *et al.* 1988). The concentrations and incubation times needed for effective metabolic inhibition via BESA and MoO_4^{-2} were determined experimentally (*data not shown*). BESA was added ~12 days prior and MoO_4^{-2} was added 12 hours prior to the start of each butyrate degradation assay to allow the inhibition to take effect.

After butyrate and inhibitor additions, gas samples were taken from the microcosm headspace approximately every other day for ~7 days using the methods described above. After each headspace gas sample was taken, 1 ml of slurry was sampled using a needle and syringe. pH was measured and then the sample was filtered (0.22-µm pore size) and stored frozen (-20ºC). The concentrations of butyrate, acetate, formate, and SO_4^{-2} were later determined using a Dionex ICS-5000+ ion chromatograph (Thermo Scientific Inc.; Waltham, Massachusetts, USA) equipped with a Dionex IonPac™ AS11-HC analytical column (2 × 250 mm) with the following elution gradient: 1 mM KOH from 0-8 min, a ramp from 8-30 mM KOH from 8-28 min, then a ramp from 30-60 mM KOH from 28-35 min. The ion chromatography results were interpreted using Chromeleon® Chromatography Data System version 7.2.0.3765.

Calculations and statistics

Gas production data

For each microcosm at each sampling point, total CH_4 production was calculated as the sum of gaseous and dissolved CH_4. The latter parameter was determined using the measured headspace CH_4 partial pressure and Henry's law. Total CO_2 production rates

were calculated in a similar way using the measurements of slurry pH to account for speciation between dissolved carbonate and bicarbonate. Rates of total CH_4 production and total CO_2 production were then calculated using linear regression; samples for which $r^2 < 0.85$ were excluded from the final dataset. These CH_4 and CO_2 production rates were summed to estimate total carbon mineralization rates, and the fraction of total carbon mineralized due to methanogenesis was also calculated (CH_4 / (CH_4 + CO_2).

Treatment effects for bulk soil slurries

Analysis of variance (ANOVA) was used to test for treatment effects on gas production data, methanogen community abundances, and salinities. Because preliminary comparisons of individual treatments across sampling events (e.g., CO_2 production rates for the fresh control at the "intrusion" and "recovery" sampling events) revealed few significant differences, data from the “intrusion” and “recovery” sampling events were combined for this analysis. Whenever a significant ANOVA result was obtained (α = 0.05), Tukey’s HSD test was used for *post hoc* comparisons. All statistical analyses were performed using JMP® Pro, version 12.2.0 (SAS Institute Inc., Cary, North Carolina, USA), with the exception of the principal component analysis described below.

Butyrate assays

The use of metabolic inhibitors in our butyrate assays allowed us to examine activity of various microbial functional groups (Fig. 1). This was accomplished by monitoring the loss of butyrate and the concurrent production of acetate, formate, CO_2, and CH_4 for seven days. Results are presented as the proportion of carbon found in each

form on each sampling day, relative to the total measured at start of the assay. When the sum of carbon in butyrate, acetate, formate, CO_2, and CH_4 was less than the total carbon measured at the start of the assay, this unaccounted portion was designated as unknown (Table 1). Single-factor ANOVA and Tukey's HSD *post hoc* tests were used to statistically compare these data for day 7. In addition, the day 7 data were subjected to principal component analysis (PCA) in order to visualize overall changes in the distribution of the major carbon compounds across treatments. Separate PCAs were performed for the "intrusion" and "recovery" sampling events using the normalized variance-covariance matrix in the PAST statistical package (Version 3, Hammer *et al.* 2001). Lastly, we calculated the rate of butyrate degradation across the entire assay period using linear regressions; samples for which $r^2 < 0.85$ were excluded from the final dataset.

RESULTS

Initial sampling event

Analysis of the bulk soil slurries for the "initial" sampling event indicate that the CH_4 production rate (0.12 ± 0.02 μmol hr^{-1}, mean ± standard error) was ~5.6% of the total carbon mineralization rate (2.2 ± 0.1 μmol hr^{-1}). There was no measurable butyrate in these microcosms and negligible concentrations of acetate (3.6 ± 0.3 μM) and formate (2.8 ± 0.2 μM). The soil was slightly acidic (6.5 ± 0.1) with a salinity of 0.28 ± 0.03 PSU (conductivity of 0.6 ± 0.1 mS cm^{-1}) and a low porewater sulfate concentration (< 0.04 mM). The abundance of archaea *16S rRNA* genes was 2.8 (± 0.2) × 10^5 copies per ng of DNA and the MST:Archaea ratio was 0.75 ± 0.05.

In the butyrate assays that did not include any metabolic inhibitors (Table 1), the rate of butyrate loss was fairly linear with 9.1 ± 0.1 % being removed each day. After 7 days of incubation, 29% of the original carbon remained as butyrate with the balance forming acetate (20%), formate (3%), CO_2 (18%), and CH_4 (19%). There was a fraction unaccounted for (11%), which likely remained in microbial biomass.

Similar rates of butyrate loss (8.8 ± 0.2 % day^{-1}) were observed when H_2 additions were used to inhibit syntrophic bacteria. At the end of these assays, 31% of the original carbon measured remained as butyrate, while the other measurable amounts remained as acetate (20%), formate (2%), CO_2 (9%), or CH_4 (17%).

In contrast, butyrate assays with added BESA showed a very different pattern of product accumulation. Methanogenesis was suppressed, as intended, and only ~0.5% of the carbon added at the start of the assay was convert to CH_4. Most of the butyrate remained (82%), with some modest accumulation of acetate (7%) and CO_2 (9%). A negligible amount as formate was also produced (~0.5 %). Even though formate was always a small fraction of the total carbon in the butyrate assays, significantly more formate accumulated when rates of butyrate breakdown were high (no inhibitor and H_2 addition microcosms) than when methanogenesis was inhibited using BESA (Fig. 3A).

Intrusion and recovery in bulk soil slurries

Measurements of the bulk soil slurries during the "intrusion" and "recovery" sampling events were pooled to analyze the effect of SRB and to determine the ability of the soil slurries to recover in terms of gas production and archaea abundance (Fig. 4). During this time, slurry salinity in the fresh controls (0.3 PSU, 0.6 mS cm^{-1}) was

significantly (ANOVA $p < 0.05$) lower compared to the other treatments (SO_4^{-2} treatment: 0.5 PSU, 1.0 mS cm^{-1}; recovery and NaCl treatments: 0.6 PSU, 1.2 mS cm^{-1}) with little variability across sampling events or between replicate microcosms (all standard errors <0.01 PSU, < 0.01 mS cm^{-1}).

Methane production was suppressed in all three treatments relative to the fresh control microcosms (Fig. 4A; $p < 0.05$). The effect was much greater when SO_4^{-2} was added to stimulate SRB activity (~80% decrease) compared to the NaCl additions (32%), where ionic strength but not SO_4^{2-} availability was altered. In microcosms recovering from stimulated SRB activity, the CH_4 production remained reduced by ~50% compared to fresh control microcosms and reduced by ~22% compared to NaCl treatment microcosms (Fig. 4A; $p = 0.09$).

Treatment effects on CO_2 production rates were more modest (Fig. 4A). The addition of SO_4^{-2} increased CO_2 production by 24% relative to the fresh control microcosms, whereas changes in ionic strength associated with NaCl addition decreased CO_2 production but the effect was not statistically significant. As with CH_4 production, partial recovery of CO_2 production was evident. Rates decreased to a level between that of the microcosms with stimulated SRB activity and the fresh controls, but were not significantly different from either.

The abundance of archaeal *16S rRNA* genes did not vary significantly across treatments (ANOVA $p=0.47$; Fig. 4B). However, the relative abundance of acetoclastic methanogens, represented using the MST:Archaea ratio, increased with stimulated SRB activity (SO_4^{-2} treatment: 0.78 ± 0.05 versus fresh control: 0.57 ± 0.04; $p<0.05$). After

SRB were inhibited for 28 days, the ratio (recovery treatment: 0.66 ± 0.03) decreased some but was not significantly different from any of the other treatments.

Butyrate breakdown during intrusion sampling event

There were three experimental treatments at the time of the "intrusion" sampling event: fresh control, NaCl treatment, and SO_4^{-2} treatment (Fig. 2). Butyrate was added to triplicate microcosms of each type, and the relative abundance of the various carbon compounds was tracked for 7 days (Table 1). In the SO_4^{-2} treatment, where SRB activity had been stimulated, the rate of butyrate loss increased by 60% (SO_4^{-2} treatment: 13.1 ± 0.1 % loss of original measured C day^{-1}) compared to all microcosms without stimulated SRB (average 8.2 ± 0.2% day^{-1}; ANOVA, $p < 0.05$). In addition, stimulating SRB activity resulted in a third less CH_4 production (SO_4^{-2} treatment: 9%; fresh control 13%; Table 1) and three times more CO_2 production (SO_4^{-2} treatment: 55%; fresh control: 19%) relative to the fresh control microcosms (ANOVA, $p<0.05$). The portion of formate in the microcosms (Fig. 3B) with increased SRB showed a pattern similar to the fresh controls until ~day 7 when it dropped to <0.7% (attributed to butyrate depletion).

For the SO_4^{-2} treatment, two additional butyrate assays were set up to help disentangle the relative activity of methanogens (inhibited by BESA addition, Table 1) and SRB (inhibited by MoO_4^{-2}, Table 1). The inhibition of methanogens caused the rate of butyrate loss to decrease 22% (to 10.1 ± 0.4% day^{-1}; ANOVA, $p<0.05$), and production of CH_4 to essentially stop (SO_4^{-2} treatment & BESA: <0.2%; Table 1). The inhibition of methanogens also resulted in a decrease in CO_2 production by approximately half (SO_4^{-2} treatment & BESA: 25%; SO_4^{-2} treatment: 54%; Table 1), and dramatically

less formate accumulated throughout the incubation (SO_4^{-2} treatment & BESA < 0.6 %; ANOVA, $p<0.05$; Fig. 3B). The MoO_4^{-2} inhibition of SRB in the SO_4^{-2} treatment during the butyrate assays caused butyrate loss to decrease by 40% (SO_4^{-2} treatment: 13.1 ± 0.1 % loss of original measured C day^{-1}; SO_4^{-2} treatment & MoO_4^{-2}: 7.8 ± 0.1 % loss of original measured C day^{-1}). The inhibition of SRB also resulted in a decrease in CO_2 by approximately half (SO_4^{-2} treatment & MoO_4^{-2}: 28%; SO_4^{-2} treatment: 54%; Table 1) but no change in CH_4 accumulation (SO_4^{-2} treatment & MoO_4^{-2}: 10%; SO_4^{-2} treatment: 9%).

Similar additions of MoO_4^{-2} to microcosms from the fresh control treatment yielded few differences in the profile of carbon compounds produced compared to the butyrate assays for either the fresh control or the NaCl treatment (Table 1). This helps confirm that the changes brought on by the MoO_4^{-2} addition were directly related to a change in activity of SRB.

Butyrate breakdown during recovery sampling event

At the "recovery" sampling event, the results of the butyrate assays for the fresh control, NaCl treatment, and SO_4^{-2} treatment were mostly similar to what was observed at the "intrusion" sampling (Table 1). The rate of butyrate loss in microcosms with stimulated SRB activity remained high (SO_4^{-2} treatment: 11.7 ± 0.1 % day^{-1}) compared to microcosms that had never received a SO_4^{-2} addition (fresh control and NaCl treatment: 8.2 ± 0.1% day^{-1}; ANOVA, $p<0.05$). Stimulated SRB activity still resulted in less CH_4 production (SO_4^{-2} treatment: 9 %; fresh control 15%) and more CO_2 production (SO_4^{-2} treatment: 51 %; fresh control 22%) than in the fresh control microcosms (ANOVA, $p <$

0.05). However, by the time of the recovery sampling event, stimulated SRB activity had resulted in ~50% less formate (SO_4^{-2} treatment: 1.2 %; fresh control 2.2%; Fig. 3C).

In microcosms recovering from stimulated SRB activity (i.e., "recovery" treatment, in which SRB were exposed to MoO_4^{-2} for 28 days), the rate of butyrate loss was ~8% less than microcosms that had never received a SO_4^{-2} addition (Recovery treatment: 7.5 ± 0.2 % day^{-1}, fresh control: 8.1 ± 0.1% day^{-1}, and NaCl treatment: 8.2 ± 0.0% day^{-1}; ANOVA, $p<0.06$). The accumulation of carbon components in this treatment differed from both the microcosms with stimulated SRB activity and those without (fresh control and NaCl microcosms; Table 1). Microcosms recovering from stimulated SRB activity had higher rates of formate accumulation (Fig. 3C) compared to all other treatments. Microcosms recovering from stimulated SRB activity did not produce significantly more or less CH_4 than either microcosms with stimulated SRB activity or fresh controls (Table 1). However, microcosms recovering from SRB activity did produce more CO_2 than fresh control microcosms and less than microcosms with stimulated SRB activity.

Principal component analysis

The PCA was used to help visualize the differences in the distribution of carbon compounds across the different microcosms at the end of each butyrate assay. For the intrusion sampling event (Fig. 5A, 84% of total variance explained), microcosms clustered into three distinct groups. Microcosms without active SRB were all characterized by greater butyrate, formate, and CH_4. Microcosms with active SRB but inhibited methanogens (BESA addition) comprised another group with decreased CH_4

production and increased acetate accumulation. Microcosms with active SRB and no inhibitor comprised the third group, which had the highest levels of butyrate breakdown and the greatest accumulation of CO_2.

For the recovery sampling, microcosms also separated into three different groups indicating differences in how the soil microbial community was metabolizing the butyrate additions (Fig. 5B, 93% of total variance explained). The first group included microcosms actively experiencing increased SRB competition (SO_4^{-2} treatment; blue circles) and is characterized by less butyrate, formate, and CH_4 and more acetate and CO_2. The second group was comprised of microcosms that did not experience SO_4^{-2} additions (fresh control and NaCl treatment; green and brown circles) is characterized by greater CH_4 and less CO_2 accumulation. The third is comprised of microcosms that had experienced increased SRB competition but for which SRB competition had been removed, either over the recovery time period (recovery treatment; purple circles) or as part of the butyrate assay (SO_4^{-2} treatment with MoO_4^{-2} additions; blue checkered filled squares). This third cluster was characterized by a relatively lower rate of butyrate degradation, greater accumulation of formate and CO_2, and a decreased accumulation of CH_4 and acetate.

DISCUSSION

The current framework for understanding how saltwater intrusion affects methanogenesis in tidal freshwater wetlands mainly considers how increased SRB activity will impact methanogens based on substrate free energy yields. This framework largely neglects how SRB activity may affect broader carbon mineralization pathways

and disrupt the tightly coupled microbial interactions that govern methane production (e.g., syntroph-methanogen interactions and competition for fatty-acids). This study begins to address these undetermined effects and demonstrates that SRB competition partially disturbs syntroph-methanogen breakdown of butyrate (i.e., a common fermentation product) in tidal freshwater wetland systems. This is also reflected in an increase in the proportion of the methanogenic community that does not participate in tightly coupled syntrophy (i.e., acetoclastic methanogens).

In addition, this work examines the ability of methanogenesis and carbon mineralization pathways to recover after saltwater intrusion has receded, which is relevant given tidal freshwater wetland systems will likely experience sea level rise as an increase in the frequency and duration of saltwater intrusion events rather than a simple steady increase in salinity. Although we found syntrophic butyrate breakdown largely recovered following the removal of SRB competition, there was an alteration to the accumulation of byproducts from syntrophic butyrate breakdown and incomplete recovery in terms of the contribution of methanogenesis to total carbon mineralization. These results indicate that, even after increased SRB activity has abated, intrusion events may have lasting effects on carbon mineralization pathways.

Syntrophy in Tidal Freshwater Wetlands

Syntrophic bacteria are able to metabolize fatty acids like butyrate because the concentration of breakdown products, specifically formate or H_2, is kept below inhibitory concentrations via methanogen consumption. This syntroph-methanogen cooperation appears to be very important in our study system. When methanogens were inhibited,

only a small fraction of added butyrate was metabolized, whereas slurries with active methanogens readily consumed butyrate (Table 1). Interestingly, addition of excess H_2 to the slurries with active methanogens did not suppress syntrophic butyrate breakdown (Table 1), which suggests H_2 was not the main electron carrier for these syntrophic associations. Instead, this syntrophic metabolism appeared to be mediated through the consumption of formate. If that were the case, we would expect to see little to no formate accumulate in the presence of an intact syntroph-methanogen consortia, and accumulation of formate at inhibitory levels in microcosms without active methanogens. Our data show the opposite pattern – with greater accumulation of formate in both treatments with active methanogens compared to the soils with a suppressed methanogen community (Fig. 3A) – and it is puzzling why the higher levels of formate accumulation did not limit butyrate consumption.

One possibility for these counterintuitive results is that methanogenic consumption of formate took place rapidly in microbial aggregates, which shielded syntrophs from inhibitory formate accumulation in the immediate microenvironment. Similarly, Krylova and Conrad (1998) observed limited inhibition of propionate breakdown when both formate concentrations and H_2 additions were measured well above inhibitory levels (ΔG values of +60 kJ mol^{-1}) and also hypothesized that microbial aggregates shielded syntrophic propionate degraders from inhibitory concentrations.

Response to saltwater intrusion in bulk soil slurries

Additions of SO_4^{-2} stimulated SRB activity and increased CO_2 production by ~ 25% while decreasing CH_4 production by ~80% (Fig. 4A), which is consistent with

previous studies on tidal freshwater wetlands (Weston *et al.* 2006; Neubauer *et al.* 2013; Neubauer 2013). One commonly considered explanation for the decrease in CH_4 production is that methanogen activity was suppressed due to direct competition with SRB for substrates (i.e., H_2, formate, and acetate), a hypothesis that is consistent with thermodynamic predictions based on the relative free energy yields of the two processes (Muyzer and Stams 2008). Additionally, the decrease in CH_4 production could also be an indirect response of the methanogens to competition between syntrophs and SRB. If SRB outcompete syntrophs for fermentation products, syntrophic production of H_2/formate will be limited and therefore restrict the availability of these electron donors to methanogens. While not specifically considered in this paper, anaerobic oxidation of methane may also play a role in how CH_4 and CO_2 production rates change in wetlands experiencing salinization. Further examination of syntrophic methane oxidation linked to sulfate reduction could be a valuable next step in understanding how intrusion events may shape microbial interactions and activity (Segarra *et al.* 2015).

Our results suggest that short-term saltwater intrusion events do not necessarily alter methanogen abundance but shift the composition of these communities towards acetoclastic genera (Fig. 4B). Acetoclastic methanogens do not participate in interspecies electron transfer and instead convert acetate directly to CH_4 and CO_2 without benefiting syntrophs. The increased dominance of these organisms after the SO_4^{-2} addition may represent a diversion of fermentation products away from syntrophic-methanogen consortia to SRB, and a disruption of syntroph-methanogen interactions. Additionally, the increase in the relative abundance of MST may be because acetoclastic methanogens in the family MST are more successful competitors with SRB than methanogens utilizing

H_2/formate. Methanogens in the MST family have a high affinity for acetate and have a low minimum acetate concentration threshold required for growth (Smith and Ingram-Smith 2007) making them well suited to compete with SRB (Omil *et al.* 1998; Stefanie *et al.* 1994). In contrast, SRB can quickly outcompete hydrogenotrophic methanogens for H_2/formate (Stefanie *et al.* 1994) or indirectly limit methanogens access because SRB do not produce H_2/formate when consuming fermentation byproducts if SO_4^{-2} is available (Martins and Pereira 2013). However, these competition dynamics may change over longer exposure periods (i.e., multiple months to a year). For example, Dang *et al.* (2019) found that when fresh water marsh soils were transplanted into a saltwater marsh, CH_4 production recovered significantly over 1 year and was correlated with the relative abundance of 3 orders of hydrogenotrophic bacteria that were not prevalent in either the fresh or salt marsh soils.

This study shows that increased ionic strength can also contribute to decreases in CH_4 production (Fig. 4A), though to a much lesser extent than competition with SRB. The salinity in the study site from which our soils were collected is consistently low (<0.8 mS cm^{-1} over the last 2 years, unpublished data), and it may be that the genera in the methanogen community were incapable of acclimating to the induced salinity stress. Other studies have observed either a decrease in methanogenesis (Baldwin *et al.* 2006) or no response (Chambers *et al.* 2011) to similar NaCl additions to freshwater wetland soils. The range of methanogen salinity tolerance is large (Patel and Roth 1977), and selective pressure from regular saltwater intrusion events may determine the resistance of the initial methanogen community to salinity stress.

Saltwater intrusion effects on syntrophy

Under freshwater conditions, there was significant breakdown of butyrate via the syntroph-methanogen consortia (Table 1). When SO_4^{-2} was added to stimulate SRB, the rate of potential butyrate breakdown increased by ~50% (Table 1). Although stimulated SRB activity did greatly diminish the role of syntroph-methanogen consortia in butyrate breakdown, syntroph-methanogen consortia still remained active in the face of competition from SRB, accounting for 22% of butyrate breakdown (compare butyrate loss in SO_4^{-2} treatment, when syntroph-methanogen consortia were active, and SO_4^{-2} treatment & BESA, when syntroph-methanogen consortia are inhibited). The diminished role of syntrophy in microcosms with stimulated SRB is also evident when tracking the concentration of the putative syntroph electron carrier formate; within seven days of butyrate additions the concentration was significantly less than in those microcosms without stimulated SRB activity (Fig. 3B & C). The observed contribution of the syntrophy-methanogen consortia may be exaggerated in these assays because the excess available butyrate may have decreased the competitive pressure from SRB compared to *in situ.* The diminished but persistent activity of syntrophs in the face of SRB competition is an especially important finding in respect to the resilience of butyrate metabolisms to saltwater intrusion events in tidal freshwater wetland soils. This is because *Syntrophomonas* and *Syntrophus*, the only known genera capable of syntrophic butyrate breakdown, are both obligate syntrophs (McInerney *et al.* 2008; Plugge *et al.* 2011) and must either successfully compete with SRB or go dormant during saltwater intrusion events. In contrast, other syntrophic metabolisms, such as propionate breakdown, can be performed by SRB in the genus *Syntrophobacter*, who are capable of switching from

SO_4^{-2} reduction to a syntrophic metabolism when SO_4^{-2} is absent (McInerney *et al.* 2008; Plugge *et al.* 2011); this metabolic flexibility likely provides functional stability in response to saltwater intrusion events.

In contrast with how stimulated SRB competed with syntrophs for butyrate, stimulated SRB did not appear to compete as aggressively with methanogens for acetate. In fact, stimulating SRB activity increased the concentration of acetate (Fig. 5), as has been seen in other freshwater wetland soils where SRB were not associated with acetate consumption (Achtnich *et al.* 1995). This increase in acetate availability during stimulated SRB activity may partially explain the relative increase in obligate acetoclastic methanogens (MST) in the bulk soil slurries in this experiment (Fig. 4B). In addition, when methanogens were inhibited in microcosms with stimulated SRB, the removal of acetate was significantly lower on day 3 (98% removal in SO_4^{-2} treatment decreased to 82% when BESA was added) and was ~ 50% less by ~ day 11 (data not shown) suggesting methanogens were important consumers of acetate (Supplemental Fig. 1). Given these observations, acetoclastic rather than H_2/formate-utilizing methanogens may be more resistant to saltwater intrusion events. This hypothesis is consistent with the results from Omil *et al.* (1998), who showed persistence of acetoclastic methanogens in bioreactors during stimulated SRB activity. Even after 250 days of excess SO_4^{-2} additions, methanogens were still responsible for ~50% of acetate consumption. The lack of proclivity for acetate utilization by SRB in this and other studies may be related to the relatively lower energy yield per unit SO_4^{-2} for acetate when compared to other substrates ($\Delta G^{\circ\prime}$ kJ mol^{-1} of SO_4^{-2} for acetate: -47.6; propionate: -50.26; butyrate: -55.6; formate: -

144.4; H_2: -151.9; lactate: -160.2; ΔG°' values obtained from Muyzer and Stams (2008) except formate, which was calculated by Omil *et al.* (1998)).

Recovery following saltwater intrusion

In our system, the effects of stimulated SRB activity on carbon dynamics remained evident even after the 28-day recovery period. Specifically, rates of methanogenesis in recovery microcosms remained reduced by 50% compared to fresh controls and by ~ 22% compared to the NaCl treatment (Fig. 4A, $p = 0.09$). The persistent effect of stimulated SRB activity was also evident on methanogenesis's contribution to total carbon mineralization. Methanogenesis only accounted for 4% of total carbon mineralization in recovery microcosms compared to 7-8% in the fresh control and NaCl microcosms.

The recovery of carbon dynamics from saltwater intrusion events in freshwater wetlands is poorly understood and rarely examined. The limited data available give contradictory results. For example, Helton *et al.* (2014) and Dorwick *et al.* (2006) found that methanogenesis can recover from the effects on elevated SO_4^{-2} within only a few months, whereas Gauci *et al.* (2005) reported incomplete recovery two years after the end of SO_4^{-2} exposure. Part of this discrepancy could be due to the duration (e.g., 4 weeks for Dorwick *et al.* (2006) versus 1 year for Gauci *et al.* (2005)), magnitude (e.g., 4 mM SO_4^{-2} in this study versus ~0.6 mM in Helton *et al.* (2014)), or frequency of exposure (Neubauer and Craft 2009). Regular saltwater intrusion events of low magnitude may select for syntroph and methanogen communities capable of acclimating to both increased salinity and SRB competition, while sites that experience more intermittent

intrusion events may be less resilient. The Cumberland tidal freshwater wetland syntroph and methanogen communities had not experienced a saltwater intrusion event of the magnitude simulated in this experiment for 2 years or more (salinity was consistently measured <0.8 mS cm^{-1}). This may explain why, after SRB competition was removed for ~28 days, the rate of methanogenesis (Fig. 4A) and the contribution of methanogenesis to total carbon mineralization did not fully recover and suggests that intrusion events into more pristine freshwater wetlands systems may have a persistent effect on carbon dynamics.

In contrast to our findings for methane production, the rate of potential syntrophic butyrate breakdown mostly recovered from stimulated SRB activity; butyrate loss rates were 7.5 ± 0.2 % day^{-1} in the recovery treatment compared to 8.1 ± 0.1% day^{-1} in the fresh control and NaCl treatments. The resilience of butyrate-utilizing syntrophs in tidal freshwater wetland environments is plausible given that syntrophic-methanogen consortia appeared to remain active when SRB activity was stimulated (discussed above). Interestingly, despite seeing near complete recovery of butyrate breakdown rates after SRB activity was removed, pronounced changes in the accumulation and production of butyrate-breakdown byproducts remained. This is clearly visualized by the distinct grouping of recovery treatments from fresh control microcosms on the PCA ordination (Fig. 5B) and indicates that SRB competition may have lasting effects on how the microbial community utilizes the byproducts of fatty acid breakdown. One possible explanation for the greater accumulation of formate and the more depleted acetate concentrations in recovery microcosms is persistence of the shift towards acetoclastic metabolisms observed during the saltwater intrusion event. However, the MST:Archaea

ratios (Fig. 4B) did not remain significantly elevated. Given the confined trophic nature of methanogens (i.e., the limited use of substrates) and the conservation of methanogenic metabolisms to a monophyletic group of organisms (Garcia *et al.* 2000), the methanogen community likely has little functional redundancy and the contribution of individual species may be important to overall ecosystem function and warrant more detailed examination using higher resolution techniques, such as *16s rRNA* Illumina sequencing, in understanding the effects of saltwater intrusion events (Allison and Martiny 2008; McGuire and Treseder 2010; Morrissey *et al.* 2014, Dang *et al.* 2019).

Conclusions

This work provides novel insight into the potential ecosystem-scale effects of substrate competition between SRB, methanogens, and syntrophic bacteria and informs the current understanding of how sea level rise may affect carbon cycling in freshwater wetlands. The failure of methanogenesis to fully recover from SRB activity in this microcosm experiment provides evidence that tidal freshwater wetlands may not all be resilient to saltwater intrusion events and may only slowly recover over months. However, these results should be verified in an *in situ* experiment, as microcosm experiments do not allow for the re-introduction of methanogens or other microbes from the surrounding environment. The work also shows that at SO_4^{-2} concentrations typical of the oligohaline zone, syntrophic bacteria and SRB can break down butyrate concurrently. Based on butyrate additions and the ratio of MST:Archaea 16s *rRNA* gene abundance, there is evidence that acetoclastic methanogens may be more suited to persist in environments experiencing increased saltwater intrusion events and that these events may alter carbon breakdown pathways. Future work that focuses on the entire microbial

community (e.g., functional predictions based on 16s amplicon sequencing) could yield greater insight into how these events possibly disrupts an array of syntrophic interactions (Douglas *et al*. 2020). Syntrophy, or "obligately mutualistic metabolism" as coined by Morris *et al.* (2013), is not confined to microbial metabolisms resulting in methane, but is used throughout the microbial community to survive in resource-limited environments. When examining the effects of disturbances like saltwater intrusion, it is important to not focus on microbial functional groups as isolated entities but as part of a cooperative microbial metabolism that can determine larger carbon and nutrient mineralization rates.

ACKNOWLEDGEMENTS

We would like to acknowledge Ember Morrissey, Chansotheary Dang, and Joseph Morina for suggestions when designing the experiment. We would like to thank Joseph Battistelli, Rachel Henderson, Mary Coughter, Aoife Preston Mahaney, and Jessica Hendry Nelson as well for their advice and feedback with the written manuscript.

FUNDING

This work was supported by a grant from the National Science Foundation [DEB 1355059] to RBF and SCN, and by a Rice Rivers Center Research Award to DJB. It is contribution #94 from the VCU Rice Rivers Center.

Conflicts of interest: None declared.

REFERENCES

Achtnich C, Schuhmann A, Wind T et al. Role of interspecies H_2 transfer to sulfate and ferric iron-reducing bacteria in acetate consumption in anoxic paddy soil. *FEMS Microbiol Ecol.* 1995;*16*(1):61-69.

Allison SD, Martiny JB. Resistance, resilience, and redundancy in microbial communities. *Proc Natl Acad Sci U.S.A.* 2008;*105*(Supplement 1):11512-19.

Bae J, McCarty PL. Inhibition of butyrate oxidation by formate during methanogenesis. *Appl Environ Microbiol*. 1993;*59*(2):628-30.

Baldwin DS, Rees GN, Mitchell AM et al. The short-term effects of salinization on anaerobic nutrient cycling and microbial community structure in sediment from a freshwater wetland. *Wetlands*. 2006;*26*(2);455-64.

Chambers LG, Reddy KR, Osborne TZ. Short-term response of carbon cycling to salinity pulses in a freshwater wetland. *Soil Sci Soc Am J*. 2011;*75*(5):2000-7.

Chauhan A, Reddy KR, Orgam AV. Syntrophic-archaeal associations in a nutrient-impacted freshwater marsh. *J Appl Microbiol.* 2006;*100*(1),73-84.

Conrad R, Mayer HP, Wüst M. Temporal change of gas metabolism by hydrogen-syntrophic methanogenic bacterial associations in anoxic paddy soil. *FEMS Microbiol Ecol.* 1989;*5*(4);265-73.

Conrad R. Contribution of hydrogen to methane production and control of hydrogen concentrations in methanogenic soils and sediments. *FEMS Microbiol Ecol*. 1999;*28*(3):193-202.

Conrad R. The global methane cycle: recent advances in understanding the microbial processes involved. *Environ Microbiol Rep.* 2009;*1*(5):285-92.

Dang C, Morrissey EM, Neubauer SC et al. Novel microbial community composition and carbon biogeochemistry emerge over time following saltwater intrusion in wetlands. *Glob Chang Biol.* 2019;*25*(2):549-61.

De Bok FAM, Plugge CM, Stams AJM. Interspecies electron transfer in methanogenic propionate degrading consortia. *Water Res.* 2004;*38*(6):1368-75.

Douglas GM, Maffei VJ, Zaneveld JR et al. PICRUSt2 for prediction of metagenome functions. *Nat. Biotechnol*. 2020;38(6): 685-8.

Dowrick DJ, Freeman C, Lock MA et al. Sulphate reduction and the suppression of peatland methane emissions following summer drought. *Geoderma*. 2006;*132*(3):384-90.

Dwyer DF, Weeg-Aerssens E, Shelton DR et al. Bioenergetic conditions of butyrate metabolism by a syntrophic, anaerobic bacterium in coculture with hydrogen-oxidizing methanogenic and sulfidogenic bacteria. *Appl Environ Microbiol.* 1988;*54*(6):1354-59.

Elshahed MS, McInerney MJ. Is interspecies hydrogen transfer needed for toluene degradation under sulfate-reducing conditions? *FEMS Microbiol Ecol*. 2001;*35*(2):163-9.

Ferry JG. How to make a living by exhaling methane. *Annu Rev Microbiol.* 2010;*64*:453-73.

Galand P, Yrjälä K, Conrad R. Stable carbon isotope fractionation during methanogenesis in three boreal peatland ecosystems. *Biogeosciences*. 2010;*7*:3893-900.

Garcia JL, Patel BK, Ollivier B. Taxonomic, phylogenetic, and ecological diversity of methanogenic archaea. *Anaerobe*. 2000;*6*(4):205-26.

Gauci V, Dise N, Blake S. Long-term suppression of wetland methane flux following a pulse of simulated acid rain. *Geophys Res Lett.* 2005;*32*(12), DOI: 10.1029/2005GL022544

Glissmann K, Conrad R. Fermentation pattern of methanogenic degradation of rice straw in anoxic paddy soil. *FEMS Microbiol Ecol*. 2000;*31*(2):117-26.

Hammer Ø, Harper DAT, Ryan PD. PAST: Paleontological statistics software package for education and data analysis. *Palaeontol. Electron.* 2001;*4*(1):1-9.

Helton AM, Bernhardt ES, Fedders A. Biogeochemical regime shifts in coastal landscapes: the contrasting effects of saltwater incursion and agricultural pollution on greenhouse gas emissions from a freshwater wetland. *Biogeochemistry.* 2014;*120*(1-3):133-47.

Herbert ER, Boon P, Burgin AJ et al. A global perspective on wetland salinization: ecological consequences of a growing threat to freshwater wetlands. *Ecosphere.* 2015;6(10):1-43.

Hoehler TM, Alperin MJ, Albert DB et al. Apparent minimum free energy requirements for methanogenic archaea and sulfate-reducing bacteria in an anoxic marine sediment. *FEMS Microbiol Ecol.* 2001;*38*(1):33-41.

Karlsson AE, Johansson T, Bengtson P. Archaeal abundance in relation to root and fungal exudation rates. *FEMS Microbiol Ecol.* 2012;*80*(2):305-11.

Krylova NI, Conrad R. Thermodynamics of propionate degradation in methanogenic paddy soil. *FEMS Microbiol Ecol.* 1998;*26*(4):281-88.

Liu H, Wang J, Wang A et al. Chemical inhibitors of methanogenesis and putative applications. *Appl Microbiol Biotechnol.* 2011;*89*(5):1333-40.

Lovley DR, Dwyer DF, Klug MJ. Kinetic analysis of competition between sulfate reducers and methanogens for hydrogen in sediments. *Appl Environ Microbiol*. 1982;43(6):1373-9.

Martins M, Pereira IA. Sulfate-reducing bacteria as new microorganisms for biological hydrogen production. *Int J Hydrog Energy*, 2013;*38*(28):12294-301.

McGuire KL, Treseder KK. Microbial communities and their relevance for ecosystem models: decomposition as a case study. *Soil Biol Biochem.* 2010;*42*(4):529-35.

McInerney MJ, Struchtemeyer CG, Sieber J et al. Physiology, ecology, phylogeny, and genomics of microorganisms capable of syntrophic metabolism. *Ann N Y Acad Sci.* 2008;*1125*(1):58-72.

McInerney MJ, Sieber JR, Gunsalus RP. Syntrophy in anaerobic global carbon cycles. *Curr Opin Biotechnol.* 2009;*20*(6):623-32.

Megonigal JP, Hines ME, Visscher PT. Anaerobic metabolism: linkages to trace gases and aerobic processes. In: Schlesinger WH (ed.). *Biogeochemistry*. Oxford: Elsevier-Pergamon, 2004, 317-424.

Moftakhari HR, AghaKouchak A, Sanders BF et al. Increased nuisance flooding along the coasts of the United States due to sea level rise: Past and future. *Geophys Res Lett.* 2015;*42*(22):9846-52.

Morris BE, Henneberger R, Huber H et al. Microbial syntrophy: interaction for the common good. *FEMS Microbiol Rev*. 2013;*37*(3):384-406.

Morrissey EM, Berrier DJ, Neubauer SC et al. Using microbial communities and extracellular enzymes to link soil organic matter characteristics to greenhouse gas production in a tidal freshwater wetland. *Biogeochemistry*. 2014;*117*(2-3):473-90.

Morrissey EM, Franklin RB. Evolutionary history influences the salinity preference of bacterial taxa in wetland soils. *Front microbiol* 2015;6:1013.

Muyzer G, Stams AJ. The ecology and biotechnology of sulphate-reducing bacteria. *Nat Rev Microbiol.* 2008;*6*(6):441-54.

Neubauer SC, Givler K, Valentine S et al. Seasonal patterns and plant-mediated controls of subsurface wetland biogeochemistry. *Ecology,* 2005;*86*(12), 3334-44.

Neubauer SC, Craft CB. Global change and tidal freshwater wetlands: scenarios and impacts. In: Barendregt A, Whigham D, Baldwin A (ed.). *Tidal Freshwater Wetlands*. Leiden: Backhuys Publishers, Weikersheim: Margraf Publishers, 2009, 353-366.

Neubauer SC, Franklin RB, Berrier DJ. Saltwater intrusion into tidal freshwater marshes alters the biogeochemical processing of organic carbon. *Biogeosciences*. 2013;*10*(12):8171-83.

Neubauer SC. Ecosystem responses of a tidal freshwater marsh experiencing saltwater intrusion and altered hydrology. *Estuaries Coast*. 2013;*36*(3):491-507.

Neubauer SC, Megonigal JP. Moving beyond global warming potentials to quantify the climatic role of ecosystems. *Ecosystems*. 2015;*18*(6):1000-13.

Odum WE. Comparative ecology of tidal freshwater and salt marshes. *Annu Rev Ecol Evol Syst.* 1988;147-176.

Omil F, Lens P, Visser A et al. Long-term competition between sulfate reducing and methanogenic bacteria in UASB reactors treating volatile fatty acids. *Biotechnol. Bioeng*. 1998;*57*(6);676-85.

Parkes RJ, Gibson GR, Mueller-Harvey I et al. Determination of the Substrates for sulphate-reducing bacteria within marine and esturaine sediments with different rates of sulphate reduction. *Microbiol.* 1989;*135*(1):175-87.

Patel GB, Roth LA. Effect of sodium chloride on growth and methane production of methanogens. *Can J Microbiol.* 1977;*23*(7):893-97.

Plugge CM, Zhang W, Scholten JC et al. Metabolic flexibility of sulfate-reducing bacteria. *Front Microbiol.* 2011;127, DOI: 10.3389/fmicb.2011.00081.

Poffenbarger HJ, Needelman BA, Megonigal JP. Salinity influence on methane emissions from tidal marshes. *Wetlands*. 2011;*31*(5):831-42.

Rothfuss F, Conrad R. Vertical profiles of CH_4 concentrations, dissolved substrates and processes involved in CH_4 production in a flooded Italian rice field. *Biogeochemistry*. 1992;*18*(3):137-52.

Segarra F, Schubotz F, Samarkin V, et al. High rates of anaerobic methane oxidation in freshwater wetlands reduce potential atmospheric methane emissions. *Nat Commun. 2015;*6:7477, DOI: 10.1038/ncomms8477

Sieber JR, McInerney MJ, Gunsalus RP. Genomic insights into syntrophy: the paradigm for anaerobic metabolic cooperation. *Annu Rev Microbiol.* 2012;*66*:429-52.

Smith KS, Ingram-Smith C. Methanosaeta, the forgotten methanogen?. *Trends Microbiol.* 2007;*15*(4):150-5

Stams AJ. Metabolic interactions between anaerobic bacteria in methanogenic environments. *Antonie van Leeuwenhoek*. 1994;*66*:271-94.

Stams AJ, De Bok FA, Plugge CM et al. Exocellular electron transfer in anaerobic microbial communities. *Environ Microbiol.* 2006;*8*(3):371-82.

Stams AJ, Plugge CM. Electron transfer in syntrophic communities of anaerobic bacteria and archaea. *Nat Rev Microbiol.* 2009;*7*(8):568-77.

Stefanie JOE, Visser A, Pol LWH et al. Sulfate reduction in methanogenic bioreactors. *FEMS Microbiol Rev.* 1994;*15*:119-36.

Thiele JH, Zeikus JG. Control of interspecies electron flow during anaerobic digestion: significance of formate transfer versus hydrogen transfer during syntrophic methanogenesis in flocs. *Appl Environ Microbiol.* 1988;*54*(1): 20-29.

Tobias C, Neubauer SC. "Chapter 16-Salt Marsh Biogeochemistry—An Overview." In: Gerardo MEP, Wolanski E, Cahoon DR, Hopkinson CS (ed.). *Coastal Wetlands*. Amsterdam: Elsevier, 2019, 539-596.

Tully K, Gedan K, Epanchin-Niell R et al. The invisible flood: the chemistry, ecology, and social implications of coastal saltwater intrusion. *BioScience*. 2019;*69*(5):368-78.

Weston NB, Dixon RE, Joye SB. Ramifications of increased salinity in tidal freshwater sediments: geochemistry and microbial pathways of organic matter mineralization. *J Geophys Res Biogeosci.* 2006, DOI: 10.1029/2005JG000071

Weston NB, Vile MA, Neubauer SC et al. Accelerated microbial organic matter mineralization following salt-water intrusion into tidal freshwater marsh soils. *Biogeochemistry*. 2011;*102*:135-51.

Yu Y, Lee C, Kim J et al. Group-specific primer and probe sets to detect methanogenic communities using quantitative real-time polymerase chain reaction. *Biotechnol Bioeng.* 2005;*89*(6):670-79.

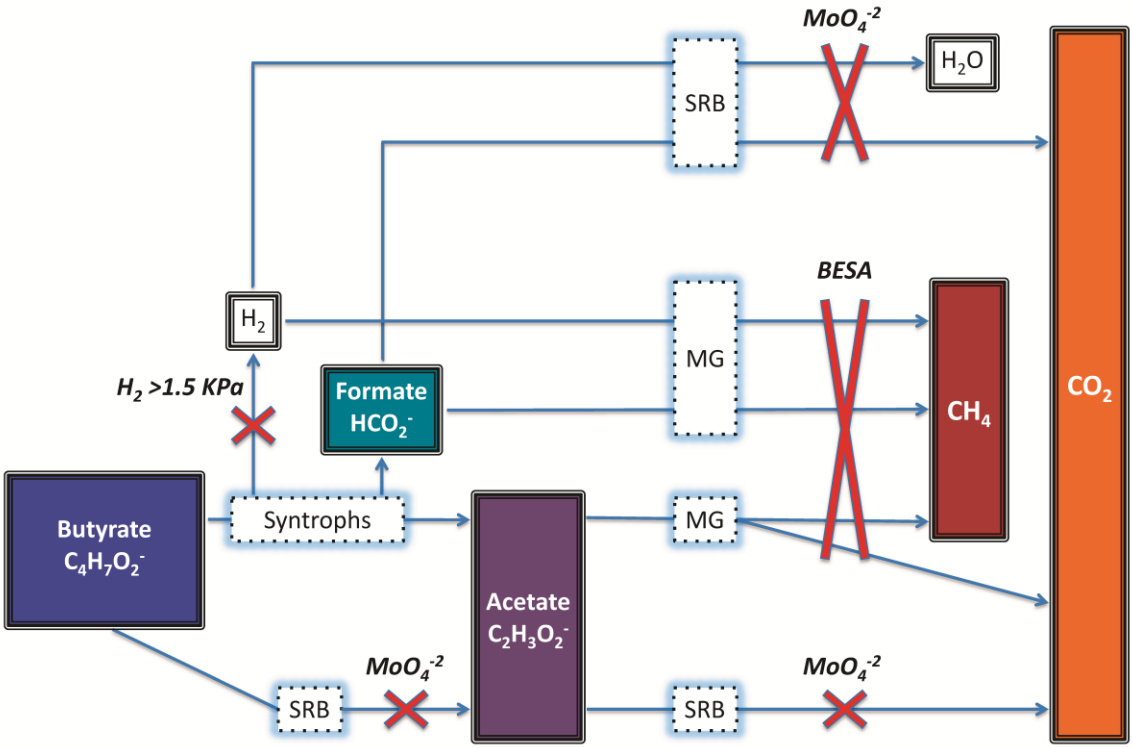

Figure 1. Pathways of butyrate breakdown in anaerobic environments, the microbial groups responsible (white boxes with dashed lines), and the steps affected by the inhibitors BESA, MoO_4^{-2}, and H_2 (red Xs). Methanogens are "MG," syntrophic bacteria are "Syntrophs," and sulfate-reducing bacteria are "SRB." The CO_2 consumption by formate formation and hydrogenotrophic methanogenesis are not included in the diagram. The production and consumption of H_2O is also not completely represented.

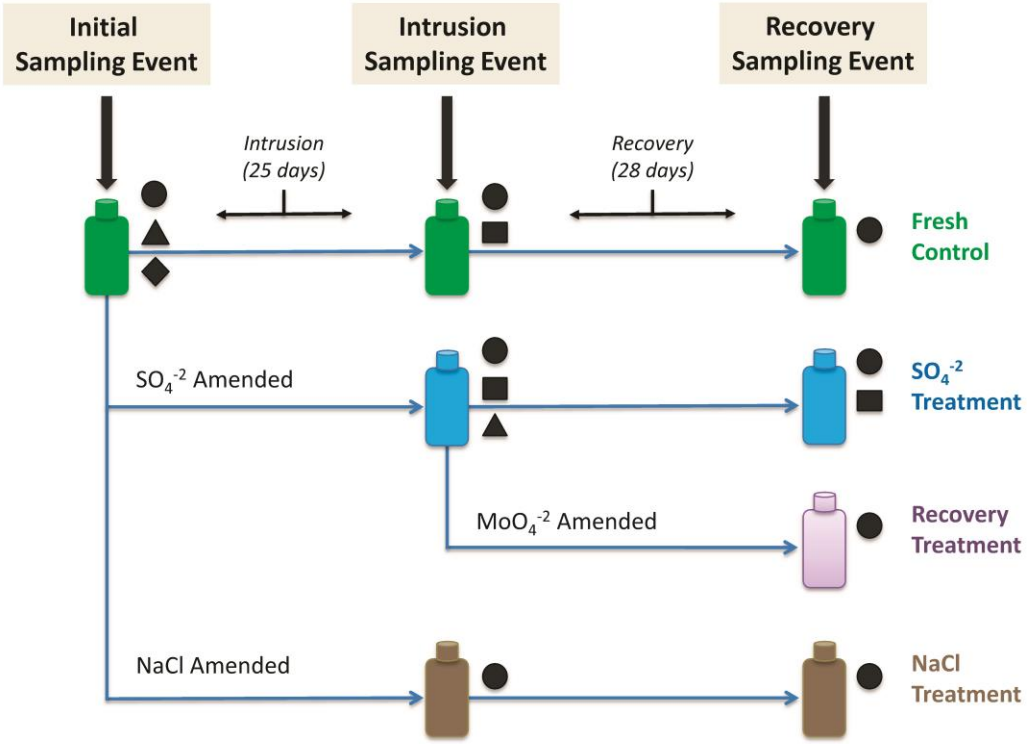

Figure 2. Summary of the treatments, incubation times, and sampling events for this experiment. Different colored bottles correspond to different treatments: green = "Fresh control" (no amendment), blue = "SO_4^{-2} treatment" (SO_4^{-2} amendments to stimulate SRB), purple = "Recovery Treatment" (SO_4^{-2} amendments to stimulate SRB, followed by MoO_4^{-2} to inhibit them), and brown = "NaCl Treatment" (NaCl amendments to mimic the ionic strength increase due to the SO_4^{-2} addition). At each sampling event, measurements were made of carbon mineralization rates (CO_2 and CH_4 production), soil pH, salinity, and archaea abundance. In addition, butyrate degradation assays were performed for each treatment group. The use of inhibitors during the butyrate assay is indicated next to each bottle: circle (●) indicates an assay performed with no inhibitor, triangle (▲) indicates an

assay performed with BESA to inhibit methanogens, diamond (◆) indicates an assay performed with H_2 to inhibit syntrophs, and square (■) indicates an assay performed with MoO_4^{-2} to inhibit SRB.

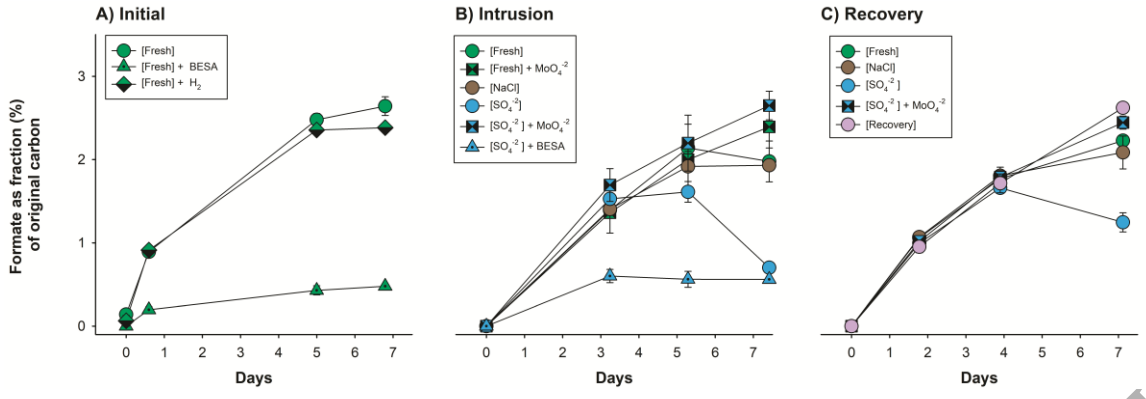

Figure 3. Mean (± standard error) of formate accumulation as a percent of the original carbon measured at the beginning of the butyrate breakdown assays. Data presented separately for the initial (A), intrusion (B), and recovery (C) sampling events. Figure legends show microcosm treatments in brackets followed by the inhibitors used in the butyrate assays.

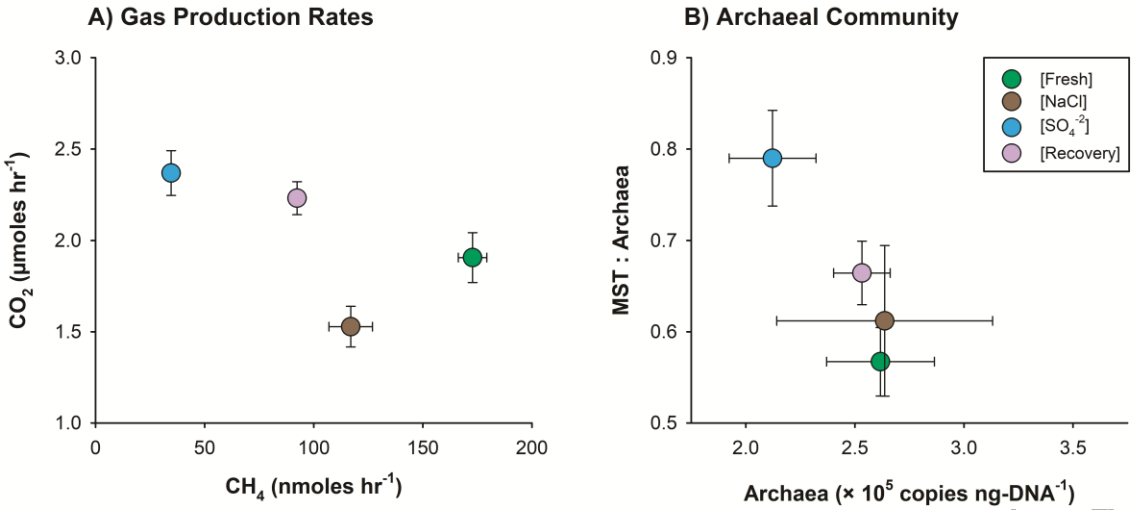

Figure 4. Mean (± standard error) gas production rates (A) and Archaea community data (B) pooled for the intrusion and recovery sampling events. Figure legends show microcosm treatments in brackets.

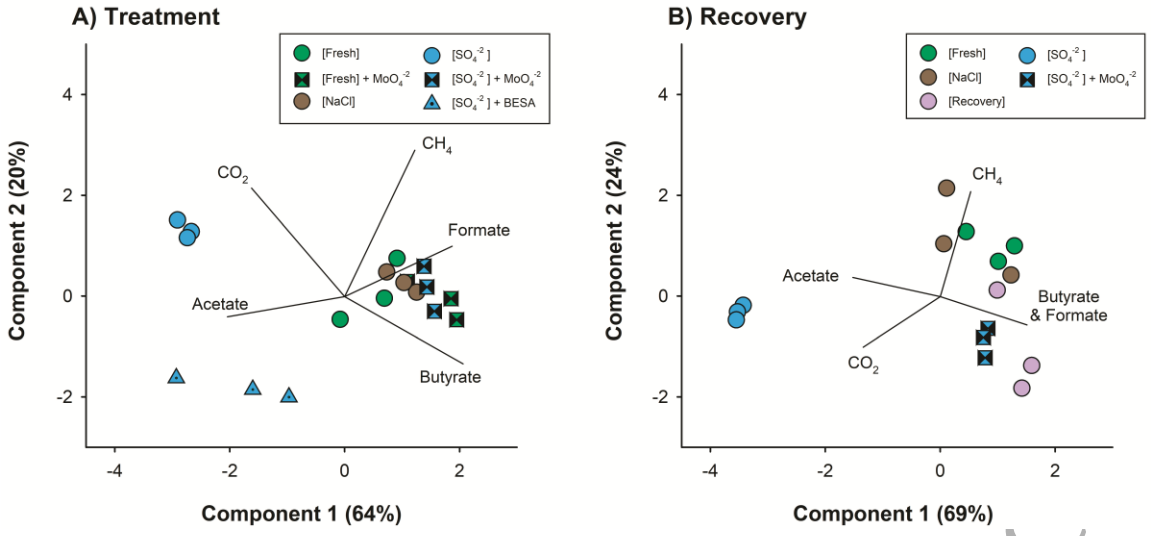

Figure 5. Principal components analysis applied to the distribution of carbon substrates (butyrate, acetate, formate, CO_2, and CH_4) in microcosms on day 7 of butyrate degradation assays. Data presented separately for the intrusion sampling (A) and the recovery (B) sampling event. Figure legends show microcosm treatments in brackets followed by the inhibitors used in the butyrate assays.

Table 1. Results of the butyrate assays (mean ± standard error). Butyrate loss rate was calculated via linear regression applied to the entire assay period; carbon distributions (%) are presented for only the final sampling point (day 7). Data for individual carbon compounds were normalized to the total measured carbon at the start of the assay. Superscript letters indicate a significant difference in the fraction of the carbon compound between treatment-inhibitor combinations within each sampling event (Tukey's HSD tests following ANOVA, $p < 0.05$).

Sampling Event	Treatment	Inhibitor	Butyrate loss (% per day)	Carbon distribution (%) at the end of the assay period					
				Butyrate	Acetate	Formate	CO_2	CH_4	Unknown
Initial	Fresh control	None	9.1 ± 0.1 ^{A}	29.5 ± 1.5 ^{A}	20.2 ± 0.8 ^{A}	2.6 ± 0.1 ^{A}	17.6 ± 0.3 ^{A}	18.6 ± 1.0 ^{A}	11.4 ± 1.6 ^{A}
	Fresh control	H_2	8.8 ± 0.1 ^{A}	31.5 ± 0.9 ^{A}	20.1 ± 0.5 ^{A}	2.4 ± 0.0 ^{A}	9.0 ± 0.4 ^{B}	17.5 ± 1.4 ^{A}	19.6 ± 1.4 ^{B}
	Fresh control	BESA	0.4 ± 0.7 ^{B}	81.7 ± 0.7 ^{B}	7.3 ± 0.2 ^{B}	0.3 ± 0.2 ^{B}	9.2 ± 1.3 ^{B}	0.3 ± 0.0 ^{B}	1.2 ± 2.2 ^{C}
Intrusion	Fresh control	None	8.5 ± 0.1 ^{A}	24.4 ± 0.5 ^{AB}	18.1 ± 0.6 ^{ABC}	1.3 ± 0.7 ^{AB}	18.8 ± 1.3 ^{A}	12.9 ± 1.0 ^{A}	24.5 ± 2.8 ^{AB}
	Fresh control	MoO_4^{-2}	8.0 ± 0.1 ^{A}	32.8 ± 4.6 ^{A}	9.3 ± 1.1 ^{C}	2.4 ± 0.3 ^{A}	22.7 ± 1.7 ^{ABC}	9.8 ± 0.4 ^{B}	23.0 ± 4.0 ^{AB}
	NaCl	None	8.6 ± 0.1 ^{A}	25.0 ± 2.0 ^{AB}	15.3 ± 0.9 ^{BC}	1.9 ± 0.0 ^{AB}	19.3 ± 1.2 ^{AB}	12.8 ± 0.1 ^{A}	25.7 ± 1.5 ^{AB}
	SO_4^{-2}	None	13.1 ± 0.1 ^{C}	0.0 ± 0.0 ^{C}	26.6 ± 1.1 ^{AB}	0.7 ± 0.0 ^{B}	54.6 ± 1.1 ^{D}	8.9 ± 0.5 ^{B}	9.2 ± 2.5 ^{C}
	SO_4^{-2}	MoO_4^{-2}	7.8 ± 0.1 ^{A}	33.6 ± 1.7 ^{A}	11.5 ± 0.9 ^{C}	2.6 ± 0.2 ^{A}	28.5 ± 1.8 ^{C}	9.6 ± 0.7 ^{B}	14.1 ± 2.1 ^{BC}
	SO_4^{-2}	BESA	10.1 ± 0.4 ^{B}	17.7 ± 4.3 ^{B}	27.3 ± 5.6 ^{A}	0.6 ± 0.0 ^{B}	26.0 ± 1.7 ^{BC}	0.2 ± 0.0 ^{C}	28.3 ± 3.2 ^{A}
Recovery	Fresh control	None	8.1 ± 0.1 ^{AB}	38.7 ± 3.1 ^{A}	16.0 ± 0.7 ^{A}	2.2 ± 0.1 ^{AB}	22.4 ± 0.6 ^{A}	14.9 ± 0.5 ^{A}	5.6 ± 1.8 ^{AB}
	Recovery	None	7.5 ± 0.2 ^{A}	45.9 ± 4.0 ^{A}	9.7 ± 0.9 ^{B}	2.6 ± 0.0 ^{A}	32.1 ± 1.4 ^{BC}	10.0 ± 2.1 ^{AB}	-0.3 ± 1.1 ^{AB}
	NaCl	None	8.2 ± 0.0 ^{B}	33.6 ± 4.4 ^{A}	17.2 ± 0.5 ^{A}	2.1 ± 0.2 ^{B}	23.5 ± 2.5 ^{AC}	15.1 ± 1.8 ^{A}	8.5 ± 1.9 ^{A}
	SO_4^{-2}	None	11.7 ± 0.1 ^{C}	13.6 ± 0.8 ^{B}	31.7 ± 2.0 ^{C}	1.2 ± 0.1 ^{C}	50.8 ± 1.5 ^{D}	8.8 ± 0.3 ^{B}	-6.1 ± 3.6 ^{B}
	SO_4^{-2}	MoO_4^{-2}	7.7 ± 0.0 ^{AB}	43.8 ± 0.6 ^{A}	12.8 ± 0.8 ^{AB}	2.4 ± 0.1 ^{AB}	34.5 ± 3.2 ^{B}	10.2 ± 0.5 ^{AB}	-3.7 ± 4.0 ^{AB}